Received: 19 October 2017 | Accepted: 21 November 2017

DOI: 10.1111/gcb.14037

PRIMARY RESEARCH ARTICLE

WILEY Global Change Biology

Trees tolerate an extreme heatwave via sustained transpirational cooling and increased leaf thermal tolerance

John E. Drake[1,2] | Mark G. Tjoelker[1] | Angelica Vårhammar[1] | Belinda E. Medlyn[1] | Peter B. Reich[1,3] | Andrea Leigh[4] | Sebastian Pfautsch[1] | Chris J. Blackman[1] | Rosana López[1,5] | Michael J. Aspinwall[1,6] | Kristine Y. Crous[1] | Remko A. Duursma[1] | Dushan Kumarathunge[1] | Martin G. De Kauwe[7] | Mingkai Jiang[1] | Adrienne B. Nicotra[8] | David T. Tissue[1] | Brendan Choat[1] | Owen K. Atkin[9] | Craig V. M. Barton[1]

[1]Hawkesbury Institute for the Environment, Western Sydney University, Penrith, NSW, Australia

[2]Forest and Natural Resources Management, SUNY-ESF, Syracuse, NY, USA

[3]Department of Forest Resources, University of Minnesota, St Paul, MN, USA

[4]School of Life Sciences, University of Technology Sydney, Broadway, NSW, Australia

[5]PIAF, INRA, Université Clermont Auvergne, Clermont-Ferrand, France

[6]Department of Biology, University of North Florida, Jacksonville, FL, USA

[7]ARC Centre of Excellence for Climate Extremes, University of New South Wales, Sydney, NSW, Australia

[8]Division of Ecology & Evolution, Research School of Biology, The Australian National University, Canberra, ACT, Australia

[9]ARC Centre of Excellence in Plant Energy Biology, Research School of Biology, The Australian National University, Canberra, ACT, Australia

Correspondence
John E. Drake, Forest and Natural Resources Management, SUNY-ESF, Syracuse, NY, USA.
Email: jedrake@esf.edu

Funding information
Australian Research Council Discovery, Grant/Award Number: DP140103415; New South Wales Climate Action Grant, Grant/Award Number: NSW T07/CAG/016; Hawkesbury Institute for the Environment; Western Sydney University

Abstract

Heatwaves are likely to increase in frequency and intensity with climate change, which may impair tree function and forest C uptake. However, we have little information regarding the impact of extreme heatwaves on the physiological performance of large trees in the field. Here, we grew *Eucalyptus parramattensis* trees for 1 year with experimental warming (+3°C) in a field setting, until they were greater than 6 m tall. We withheld irrigation for 1 month to dry the surface soils and then implemented an extreme heatwave treatment of 4 consecutive days with air temperatures exceeding 43°C, while monitoring whole-canopy exchange of CO_2 and H_2O, leaf temperatures, leaf thermal tolerance, and leaf and branch hydraulic status. The heatwave reduced midday canopy photosynthesis to near zero but transpiration persisted, maintaining canopy cooling. A standard photosynthetic model was unable to capture the observed decoupling between photosynthesis and transpiration at high temperatures, suggesting that climate models may underestimate a moderating feedback of vegetation on heatwave intensity. The heatwave also triggered a rapid increase in leaf thermal tolerance, such that leaf temperatures observed during the heatwave were maintained within the thermal limits of leaf function. All responses were equivalent for trees with a prior history of ambient and warmed (+3°C) temperatures, indicating that climate warming conferred no added tolerance of heatwaves expected in the future. This coordinated physiological response utilizing latent cooling and adjustment of thermal thresholds has implications for tree tolerance of future climate extremes as well as model predictions of future heatwave intensity at landscape and global scales.

KEYWORDS
climate change, *Eucalyptus parramattensis*, heatwave, latent cooling, photosynthesis, temperature, thermal tolerance, warming

1 | INTRODUCTION

Heatwaves are a regular climate component in many areas of the world, consisting of several consecutive days of extreme temperatures and a dry atmosphere, often combined with dry surface soils (Teskey et al., 2015). Several extreme heatwaves have recently been observed in Europe, Australia, and China, with strong negative effects on ecosystem C uptake (Ciais et al., 2005; van Gorsel et al., 2016; Yuan et al., 2016). Earth system models used in the fifth model intercomparison project (CMIP5) predict that heatwave amplitude—a proxy of heatwave intensity—will increase by up to 4.8°C for RCP8.5 (2081–2100 vs. 1950–2005; Cowan et al., 2014). The CMIP5 multimodel ensemble also projects increases in heatwave frequency (1.7 ± 6.6 per decade to 13.0 ± 27 per decade under RCP8.5, 2006–2016 vs. 2090–2100). Heatwaves occur against a backdrop of a gradual increase in mean temperature (+0.85°C globally from 1880 to 2012, +1°C for Australia from 1910 to 2016) that is predicted to reach +3°C by 2100 (Australian Bureau of Meteorology State of the Climate Report, 2016; IPCC, 2014). Thus, climate change is predicted to increase the intensity and frequency of heatwaves, along with a gradual increase in mean temperature.

The response of trees to extreme heatwaves is uncertain but important for ecosystem function (Allen, Breshears, & McDowell, 2015; Ciais et al., 2005; van Gorsel et al., 2016; Reichstein et al., 2013; Teskey et al., 2015). Some ecological processes are more sensitive to changes in extremes than to changes in mean values (Frank et al., 2015; Hansen, Sato, & Ruedy, 2012). For example, extreme temperatures combined with prolonged drought have been implicated as drivers of forest mortality (Allen et al., 2010, 2015). High temperatures during extreme heatwaves may exceed plant thermal thresholds, leading to direct thermal damage or mortality (O'Sullivan et al., 2017) unless plants can quickly adjust to these extreme conditions. We have known for some time that plants can quickly produce heat-shock proteins that can ameliorate thermal damage of heat treatments (e.g., Colombo & Timmer, 1992; Gifford & Taleisnik, 1994). However, it is not clear whether rapid physiological adjustments in thermal tolerance occur in response to heatwaves in the field, or whether this is an effective protectant during the extreme heatwaves that are predicted to occur in the future (O'Sullivan et al., 2017). Furthermore, plants adjust many aspects of their physiology in response to long-term changes in air temperature (T_{air}), a process termed physiological acclimation (Reich et al., 2016; Smith & Dukes, 2013; Yamori, Hikosaka, & Way, 2014). However, it is not known whether acclimation to long-term warming modifies a tree's physiological performance in an extreme heatwave (Teskey et al., 2015).

A further key unknown relates to the regulation of CO_2 and H_2O exchange during extreme heatwaves. Net rates of leaf photosynthesis often decline at high temperatures because of increased mitochondrial respiration, photorespiration, impairments to photosynthetic biochemistry, and stomatal closure (Lin, Medlyn, & Ellsworth, 2012; Teskey et al., 2015). During moderate environmental conditions, stomatal conductance (g_s) is effectively predicted as a function of photosynthetic rate (*A*) and vapor pressure deficit (*VPD*), which are in turn affected by temperature (Ball, Woodrow, & Berry, 1987; Leuning, 1995; Medlyn et al., 2011). Photosynthesis and transpiration are thus "coupled" via g_s. If such coupling continues under extreme heatwave conditions, when air temperatures can exceed 40°C and *VPD* can exceed 4 kPa, we would predict *A* and g_s to strongly decline toward zero such that transpiration would also decline toward zero despite the increase in *VPD*. This would increase leaf temperatures by limiting transpirational cooling, resulting in a positive feedback to regional surface temperatures by increasing the sensible heat flux (van Gorsel et al., 2016) and exacerbating the chance of direct thermal damage to leaf function (O'Sullivan et al., 2017).

It is possible, however, that *A* and g_s may decouple under extreme heatwave conditions, leading to substantial rates of transpiration despite near zero or negative *A*. Such decoupling has been observed in a few heatwave experiments with small, well-watered, potted plants (Ameye et al., 2012; von Caemmerer & Evans, 2015; Rogers et al., 2017; Urban, Ingwers, McGuire, & Teskey, 2017), but it is not clear if this is a general response that applies to large trees in the field. Such decoupling would maintain latent cooling of leaf temperatures and possibly protect against thermal damage. Decoupling may also be important as a feedback to regional temperature, as transpiration strongly impacts land surface temperatures and model predictions of heatwave intensities in future climates (Kala et al., 2016). Continued transpiration during extreme temperature and VPD conditions requires a functional plant hydraulic system, but extreme conditions may lead to hydraulic failure (e.g., Mitchell, O'Grady, Hayes, & Pinkard, 2014), particularly if soil water availability is low and water potentials drop to values that impair water transport. Thus, the coordinated physiological response of trees to extreme heatwaves is uncertain but important for tree survival, ecosystem function, and climate feedbacks in the future.

We exposed *Eucalyptus parramattensis* trees to 1 year of experimental climate warming (ambient vs. +3°C) followed by an extreme heatwave using 12 whole-tree chambers (WTCs) in Australia (Figure 1). Growing trees under current ambient and warmed temperatures enabled a test of whether warmed trees of the future are better able to cope with an extreme heatwave. We withheld irrigation for 1 month such that the surface soils were dry during the heatwave. These WTCs control T_{air}, CO_2, and VPD while measuring whole-canopy CO_2 and H_2O exchange (Barton et al., 2010; Drake et al., 2016) in an ecologically meaningful context with relatively large trees (6–9 m tall) in a field setting (Figure 1). This enabled assessment of heatwave impacts on integrated CO_2 and H_2O fluxes of trees rooted in native soil with natural diurnal cycles of solar irradiance, T_{air} and VPD, avoiding the artifacts inherent in glasshouse experiments with small potted trees. We show that these trees successfully coped with an extreme "heatwave of the future" through a rapid and integrative physiological response including: (1) photosynthetic decoupling and sustained transpirational cooling of leaves, (2) the maintenance of a functional hydraulic system, and (3) increased leaf thermal tolerance.

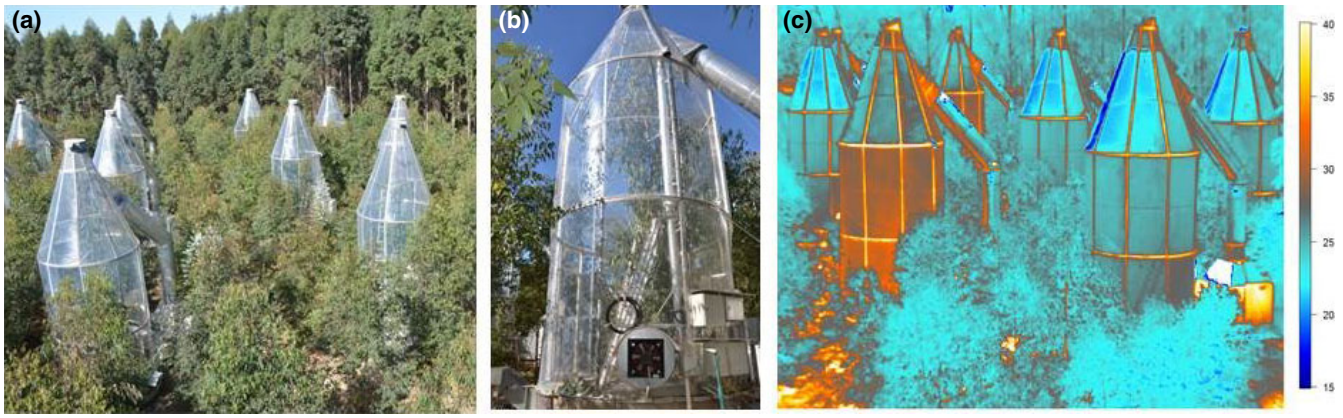

FIGURE 1 Whole-tree chambers in Richmond, New South Wales, Australia. Twelve 9 m tall chambers in a field setting (a) enclose the canopies of individual *Eucalyptus parramattensis* trees rooted in soil (b). Two heatwave chambers can be seen on the left of the infrared image, along with several control chambers (c; temperature in °C)

2 | MATERIALS AND METHODS

2.1 | Site and species description

This experiment was implemented at a site in Richmond, New South Wales, Australia (33°36′40″S, 150°44′26.5″E), using 12 WTCs. The WTCs are large cylindrical structures topped with a cone (3.25 m in diameter, 9 m in height, volume of ~53 m^3) that enclose a single tree rooted in soil. The WTCs controlled T_{air}, VPD, and atmospheric CO_2 concentration in the canopy air space while measuring the net exchange of CO_2 and H_2O for the entire canopy at 15 min resolution (Barton et al., 2010; Drake et al., 2016). The circular base of each WTC was equipped with a vertical root exclusion barrier extending approximately 1 m belowground into a hard horizontal layer of cemented manganese nodules and clay. Thus, the rooting volume of each tree was compartmentalized. Soils were an alluvial formation of low-fertility sandy loam (Drake et al., 2016). Local climate is warm; mean annual temperature is 17°C and mean annual precipitation is 720 mm.

We selected a locally endemic and threatened woodland tree species (*Eucalyptus parramattensis*) for this experiment. This species is protected by environmental legislation and is a preferred food source for koalas (Phillips, Callaghan, & Thompson, 2000). Seed was acquired from Harvest Seeds and Native Plants (Terry Hills, NSW, Australia) and germinated in a local shade house. Six potted seedlings were placed into each WTC, and the experimental warming treatment (see below) was initiated on October 28, 2015. One seedling was planted into the soil within each WTC on December 23, 2015; at that time, average seedling height was 60 cm.

2.2 | Long-term warming experiment

We implemented a warming experiment on October 28, 2015. Six chambers tracked the natural variation in T_{air} and relative humidity (RH) observed at the site; we refer to this as the "ambient" treatment. Six chambers tracked the ambient T_{air} plus 3°C while also tracking the ambient RH; we refer to this as the "warmed" treatment. This design was similar to a previous experiment with *Eucalyptus tereticornis* (Aspinwall et al., 2016; Drake et al., 2016). Prior to the heatwave, T_{air} in the ambient treatment over the 12-month period had a mean value of 15.2°C and ranged from −1.2 to 35.6°C. Tracking ambient RH in the warmed treatment resulted in a realistic simulation of future conditions of atmospheric humidity (Drake et al., 2016). All chambers tracked the ambient observed concentration of atmospheric CO_2. All trees were irrigated equally every 2 weeks at half of the mean monthly rainfall for this location until 1 month prior to the heatwave, after which irrigation was suspended.

2.3 | Heatwave experiment

We added a heatwave treatment to the long-term warming treatment, resulting in a 2 × 2 factorial design with three replicate trees in each treatment combination (n = 3). As heatwaves often occur during conditions with low soil water availability (Teskey et al., 2015), we withheld irrigation for 1 month, leading to dry surface soils during the heatwave (Figures S1–S2). We then implemented an experimental heatwave during the Austral Spring–Summer, consisting of 4 sunny days with a maximum T_{air} of 43–44°C and a maximum VPD of 5–6 kPa (Figure S3). We considered this an extreme but biologically reasonable "heatwave of the future" for this location, as the most intense heatwave on record was 4 consecutive days with a maximum T_{air} of 40–41°C (5–8 February 2009, data from 1953 to 2016) and a 3°C increase in maximum T_{air} is predicted by 2100 (Cowan et al., 2014; Sillmann, Kharin, Zwiers, Zhang, & Bronaugh, 2013). We applied this heatwave equally to trees with a history of ambient or warmed growth (+3°C) temperatures, testing whether warmed trees of the future are better able to cope with an extreme heatwave.

We defined two experimental conditions: the heatwave treatment (4 days with a maximum T_{air} of 43–44°C) and an average summer comparison condition (4 days with a maximum T_{air} of 28–29°C).

Note that this interrupted the long-term +3°C warming treatment for the 4 heatwave days. That is, the ambient control and warmed-control trees experienced equivalent conditions during the heatwave, as did the ambient heatwave and warmed-heatwave trees (Figure S3). This allows for the separation of the direct temperature effect of the heatwave from the effect of thermal history, which would not have been possible had we implemented the heatwave while maintaining the long-term +3°C treatment difference.

We implemented a dry atmosphere to simulate the hot and dry conditions typical of Australian heatwaves (Cowan et al., 2014). The observed average VPD during the heatwave was 2.16 and 4.86 kPa, and the maximum VPD values were 2.53 and 5.97 kPa in the ambient and heatwave treatments, respectively. Thus, maximum VPDs in this experiment were comparable with the 2009 heatwave (6.2 kPa). We successfully implemented an extremely dry atmosphere during the experimental heatwave.

2.4 | Whole-canopy CO_2 and H_2O flux

The WTCs used a mass-balance approach to calculate the rates of CO_2 and H_2O exchange between each tree and its canopy airspace every 15 min (Barton et al., 2010; Drake et al., 2016). Soil-derived fluxes of CO_2 and H_2O were excluded from the canopy flux measurements with a suspended plastic floor sealed around the stem of each tree at 45 cm height. To account for differences in tree size, we expressed these raw canopy fluxes on a leaf area basis by dividing by total canopy leaf area.

Total canopy leaf area was measured for each tree with a full destructive harvest on November 23, 2016. The canopy of each tree was divided into three equal heights (low-, mid-, and top-canopy thirds) and all leaves were removed from branches. A random sample of 100 leaves per canopy layer was measured for total leaf area (LI-3100C; Licor Environment, Lincoln, NE, USA), dry mass, and specific leaf area (SLA). We calculated the total leaf area of each tree as the product of layer-specific SLA and leaf dry mass summed across the three canopy layers. We assumed that total leaf area did not change substantially during the 28 days between the start of the flux data presented here (October 29, 2016) and the final harvest. We suggest that this is an appropriate assumption, given low rates of leaf formation or litterfall during this period.

2.5 | Leaf thermal tolerance

We used a measurement of the high-temperature thermal threshold of photosystem II integrity (T_{50}) as an index of leaf thermal tolerance. We measured T_{50} with an established laboratory protocol (Curtis, Knight, Petrou, & Leigh, 2014) based on the ratio of dark-adapted variable fluorescence relative to maximal fluorescence (F_v/F_m). T_{50} is the temperature at which dark-adapted F_v/F_m declines to 50% of its healthy unstressed value (Curtis et al., 2014). We measured T_{50} before the heatwave (October 19, 2016), at two time points during the heatwave (after 1 and 4 full days of heatwave temperatures) and at three time points after the heatwave (after 3, 6, and 13 days of recovery).

We sampled 12 leaves from each tree between 07:30 and 08:30 hr and transported them to a nearby laboratory in dark plastic bags humidified with moist paper towel. Leaves were separated into ~4 cm^2 discs, which were dark adapted for at least 30 min prior to a measurement of initial F_v/F_m. Three leaf discs from each tree were then exposed to a sequence of temperature treatments: (1) an initiation treatment of 15 min at 24°C, (2) a thermal stress treatment of exactly 15 min at either 24, 44, 46, 48, 50, 52, or 54°C, and (3) a recovery treatment of 90 min at 24°C. All treatments were performed at a light intensity of 500 μmol m^{-2} s^{-1}. All leaf discs were then allowed to recover overnight in the dark, and F_v/F_m was measured again. T_{50} was derived using a Weibull function fit to the F_v/F_m using the "fitplc" R package; tree-level estimates of T_{50} were obtained by fitting this function to the final overnight data collected for each tree on each date. As described previously for a range of plants (Curtis et al., 2014), the initial and overnight F_v/F_m values of leaf discs exposed to the 24°C control treatment were equivalently high (~0.8), indicating that there were no methodological artifacts related to sample handling.

2.6 | Leaf temperature

We measured leaf temperature (T_{leaf}) with continuous infrared measurements of the upper canopy ($T_{L\text{-}IR}$) and continuous thermocouple measurements ($T_{L\text{-}TC}$). An infrared radiometer (SI-111; Apogee Instruments, Logan, UT, USA, emissivity set to 0.97) was mounted inside the northern (sun facing) side of each WTC at 7 m height and pointed at an area of dense foliage in the upper third of the canopy for each tree. These sensors integrate over an area of ~1 m^2 and thus measure a canopy temperature averaged across many leaves. We refer to these data as $T_{L\text{-}IR}$.

Fine-wire thermocouples (0.13 mm diameter, Model 5SRT; Omega Engineering, Norwalk, CT, USA) were installed on the abaxial surface of two upper canopy leaves per tree. We made small holes through the abaxial epidermis with fine needles and installed the thermocouples such that the junction was inside the leaf and touching the mesophyll. This installation avoided artifactual effects of tape or glue on measured T_{leaf}. We investigated and could not find an effect of thermocouple installation on T_{leaf} as measured by a thermal camera. We refer to these thermocouple measurements as $T_{L\text{-}TC}$. We evaluated the efficacy of these measurements of leaf temperature in two focused campaigns prior to the heatwave (*see on-line supporting information*). We concluded that $T_{L\text{-}IR}$ was a reliable measure of average leaf temperature, but that individual leaf temperatures were highly variable owing primarily to variation in light in complex canopies.

2.7 | Hydraulics

To assess tree water status and hydraulic integrity, we measured predawn and midday leaf water potentials, the water potential at

turgor loss point (TLP), leaf hydraulic conductance, and branch hydraulic conductivity.

Predawn and midday leaf water potentials ($\Psi_{L\text{-}PD}$ and $\Psi_{L\text{-}MD}$) were measured prior to the heatwave (October 19, 2016), at three points during the heatwave (1st, 3rd, and 4th November of 2016), and once after the heatwave (November 7, 2016). Two leaves were measured per tree on each date using a Scholander-type pressure chamber (1505D-EXP; PMS Instrument Company, OR, USA). Leaves were placed in sealed plastic bags humidified with damp paper towel, placed in a dark cool box, and measured within 2 hr of collection in a nearby laboratory.

The water potential at which leaves lose turgor and leaf capacitance was measured using pressure–volume curves obtained with the standard bench drying approach (Tyree & Hammel, 1972). Two leaves per tree were collected prior to the heatwave (October 19, 2016) and were allowed to rehydrate overnight. The following morning they were dehydrated slowly on the benchtop, and Ψ_L and leaf mass were measured at intervals. Leaf area was measured with a scanner and analyzed with WinFOLIA (Regent Instruments, Inc., Canada). Leaf dry mass was measured after drying for 48 hr at 80°C. The TLP was estimated as the point of transition between curvilinear and linear portions of the graph of $1/\Psi_L$ vs. the relative water content. Leaf capacitance (C_{leaf}) was determined using the slope of the pressure–volume curve for each tree.

Leaf hydraulic conductivity (K_{leaf}) was measured using the kinetics of Ψ_L relaxation upon leaf rehydration (Brodribb & Holbrook, 2003). One 30–40 cm branch was collected early in the morning on the fourth day of the heatwave and transported to the laboratory in black plastic bags. Branches were cut to a length sufficient to prevent emboli from extending into the petioles of the leaves. Once in the laboratory, branches were allowed to desiccate slowly for up to 48 hr, before being carefully bagged to prevent water loss and equilibrate water potential throughout the branch. Initial Ψ_L was determined by measuring a leaf neighboring the sample leaves. Two sample leaves were then cut under water and allowed to rehydrate for 15–20 s and final Ψ_L was measured. K_{leaf} was calculated as $K_{leaf} = C_{leaf} \ln[\Psi_o/\Psi_f]/t$ where Ψ_o = initial leaf water potential (MPa); Ψ_f = final leaf water potential (MPa); t = duration of rehydration (s); C_{leaf} = leaf capacitance (mmol m^{-2} MPa^{-1}). The two values of K_{leaf} were then averaged to assess a mean K_{leaf} value for each tree at each time point.

One shoot per tree was harvested in the early morning before and just after the heatwave to assess native embolism (i.e., the loss of hydraulic conductivity). One hour before collection, shoots were covered with black plastic bags and sprayed with water to stop transpiration. Shoots were harvested under water and transported to the laboratory with their cut ends immersed in water and their leaves covered to release tension. Two 5 cm long segments were excised under water from terminal parts of each shoot and connected to a flow meter (Bronkhorst High-Tech B.V., Ruurlo, the Netherlands). Hydraulic conductance was measured at low pressure (≤ 2 kPa) before (k_i) and after (k_f) flushing with ultrapure, degassed 2 mmol KCl solution at high pressure for 30 min. Percentage loss of hydraulic conductivity (PLC) was calculated as: PLC = 100 − k_i/k_f * 100. Xylem-specific hydraulic conductivity was assessed by dividing hydraulic conductance by the sapwood area in the middle of the segment and multiplying by sample length.

2.8 | Soil water content

Soil volumetric water content was measured by six sensors permanently installed in each chamber (CS650 time-domain reflectometers; Campbell Scientific, Logan, UT, USA). Sensors were installed horizontally at three depths: four sensors were installed in the surface soil (5 cm depth) to capture spatial variation within each chamber, and single sensors were placed at 30 cm depth and just above the hard layer of cemented manganese (~90 cm depth). All sensors measured volumetric water content at 15 min resolution; we present daily averages.

We also utilized neutron-probe measurements to assess variation in soil volumetric water content throughout the soil profile, including deep soil (25–425 cm depth). A single neutron probe (503DR, Hydroprobe, Instrotek, NC, USA) was used to measure soil water content to a depth of 425 cm (at 25 or 50 cm steps) approximately every 2 weeks in each chamber (Duursma et al., 2011). Note that high neutron-probe counts in deep soil (150–400 cm depth) partially reflect a change in soil texture toward a higher clay content.

2.9 | Leaf photosynthetic modeling

We used an established leaf-level photosynthetic model (Duursma, 2015) to define our expectations for the responses of photosynthesis and transpiration to the heatwave. The model consists of three components: photosynthetic biochemistry (Farquhar, Caemmerer, & Berry, 1980), the Medlyn stomatal model linking g_s to net photosynthesis (Medlyn et al., 2011), and a leaf energy balance model (Wang & Leuning, 1998). This "big-leaf" model utilizes the same underlying components as the land surface models that are used to project future climate (Kala et al., 2016; Rogers et al., 2017; Sillmann et al., 2013; Smith & Dukes, 2013). The model has previously been shown to describe the temperature dependence of photosynthesis in a manner that was equivalent with a complex multilayer canopy model (Duursma et al., 2014). This model utilized the Medlyn et al. (2011) g_s formulation, which assumes a positive functional link between g_s and net photosynthesis in a manner similar to previous and widely used formulations (Ball et al., 1987; Leuning, 1995).

The model takes three environmental inputs: incident photosynthetic photon flux density (PPFD), VPD, and T_{air}. PPFD was measured at the top of a demountable building at the site, while VPD and T_{air} were directly measured inside the airspace of each chamber (Figure S3). We fit several model parameters to the observed temperature responses from the control treatment, as described in the online supporting information. The model was able to suitably recreate the observed A_{canopy}, E_{canopy}, and T_{leaf} in the control treatment. The root-mean-square error (RMSE) and r^2 values for predicted vs.

observed relationships were 2.1 μmol m^{-2} s^{-1} and 0.58 for A_{canopy}, 0.47 mmol m^{-2} s^{-1} and 0.61 for E_{canopy}, and 1.1°C and 0.95 for T_{leaf}. The model was also able to predict T_{leaf} as a function of T_{air} and incident PPFD in the control treatment. For example, at high light (PPFD > 1,000 μmol m^{-2} s^{-1}), observed T_{leaf} values were warmer than T_{air} by 1.6°C (standard deviation of 0.9°C), while the model-simulated values of T_{leaf} were warmer than T_{air} by 1.7°C (standard deviation of 0.2°C). Thus, the model was able to robustly simulate A_{canopy}, E_{canopy}, and T_{leaf} in the control treatment. We then applied this fitted model to the environmental data observed in the heatwave treatment and compared the model predictions of A_{canopy}, E_{canopy}, and T_{leaf} to observations during the heatwave conditions.

2.10 | Statistical analysis

The total sums of A_{canopy} and E_{canopy} during the 4-day heatwave period were analyzed as a simple 2 × 2 factorial ANOVA using the "lm" function in R (version 3.3.2). The longitudinal measurements of T_{50} were analyzed as a repeated-measures ANOVA; the chamber was included as a random effect while the warming and heatwave treatments were included as whole-plot factors, and time was a subplot factor; this analysis utilized the "lme" function of the nlme R package. There was a significant interaction between time and heatwave treatment on T_{50} ($p = .02$); we used the "phia" R package for post hoc tests regarding this interaction. The heatwave treatment was not statistically significant on the first date of measurements (preheatwave; $p > .1$), but the heatwave effect was significant on all other dates (maximum $p < .01$). Linear correlations were analyzed with the "lm" function. Note that the data and analysis code are freely available (see details in Supporting Information).

3 | RESULTS

The effects of the experimental heatwave were equivalent for trees grown under ambient and warmed (+3°C) temperatures for all measurements; there were no statistical effects of long-term warming or warming by heatwave interactions. Hence, we present the control vs. heatwave response averaged across ambient- and warm-grown trees ($n = 6$).

Canopy-averaged fluxes of photosynthetic CO_2 uptake (A_{canopy}) and transpirational H_2O loss (E_{canopy}) were equivalent for control and heatwave trees prior to the experimental heatwave (Figure 2). The heatwave treatment did not affect A_{canopy} during the moderate morning conditions, but reduced A_{canopy} by an average of 95% during the hottest period of the day (1200–1400 hr; Figure 2b). The heatwave treatment also increased respiratory CO_2 loss at night (Figure 2b). As a result, the heatwave reduced total A_{canopy} during the 4-day period by 40% (main effect of heatwave, $p < .001$; Figure 2d); this effect was equivalent for trees grown under ambient vs. warmed (+3°C) conditions prior to the heatwave (main effect of experimental warming, $p = .98$; interaction, $p = .85$). The reduction in integrated A_{canopy} was most strongly associated with reduced daytime C-uptake; increased respiratory C-loss at night played a minor role (Figure S4). Notably, A_{canopy} recovered completely on the first day following the heatwave (Figure 2b).

The heatwave treatment reduced E_{canopy} in the afternoon by an average of 33% but increased E_{canopy} at night (Figure 2c), resulting in no change in total E_{canopy} (Figure 2e; no significant effects, all $p > .05$). Importantly, these results indicate a decoupling of A_{canopy} and E_{canopy} during midday conditions of extreme T_{air} and VPD such that instantaneous water use efficiency (A_{canopy}/E_{canopy}) approached zero (Figure S5a). The heatwave trees reduced A_{canopy} to approximately zero, but maintained E_{canopy} at relatively high values (Figure S5b).

Leaves rapidly increased their high-temperature tolerance in response to the heatwave. The high-temperature threshold of photosynthetic integrity (Curtis et al., 2014; T_{50}) was high (~48.5°C) across all treatments prior to the heatwave (minimum $p > .1$), including trees designated for the control and heatwave treatment (Tukey post hoc test; $p > .1$). This is consistent with a large thermal safety margin (O'Sullivan et al., 2017). Within 24 hr of heatwave treatment, T_{50} increased by ~2°C and increased a further 1°C after 4 days to ~51°C (Figure 3a; heatwave by time interaction, $p < .01$). This 3°C change in T_{50} is a large adjustment, equivalent to a 28° latitudinal shift across a global dataset (O'Sullivan et al., 2017). The enhancement of T_{50} declined after the heatwave, but was maintained at higher levels than control trees for at least 2 weeks (Figure 3a; heatwave effect persisted on last date; Tukey post hoc test, $p < .05$). The temporal variation in T_{50} was strongly correlated with the average measured canopy temperature of the preceding day (Figure 3b). There was a hysteresis, however, as the heatwave trees maintained higher T_{50} than expected after the heatwave had passed (Figure 3a, red circle in Figure 3b).

Leaf and air temperatures (T_{leaf} and T_{air}) were strongly correlated and nearly equivalent during sunlit periods (PPFD > 500 μmol m^{-2} s^{-1}; Figure 4a). When T_{air} was 20°C, average T_{leaf} was 1.3°C warmer than T_{air}; by contrast, when T_{air} was 45°C, T_{leaf} was 0.2°C cooler than T_{air} (Figure 4b). Values of T_{leaf} were maintained below values of T_{50}, even during the heatwave (Figure 4c, d). Some leaves in the heatwave treatment approached 49–50°C, which would have exceeded the critical thermal threshold, had T_{50} not increased during the heatwave (compare histogram and vertical blue line in Figure 4c).

The continued transpiration during heatwave conditions moderated T_{leaf} via latent cooling. We parameterized a coupled photosynthetic model (Duursma, 2015) of photosynthetic biochemistry (Farquhar et al., 1980), stomatal conductance (g_s; Medlyn et al., 2011), and leaf energy balance (Wang & Leuning, 1998) based on the A_{canopy} and E_{canopy} observations in the control treatment (Figure 5a, c) and then used the model to predict A_{canopy} and E_{canopy} under heatwave conditions. This model captured the reduction in A_{canopy} with increasing T_{leaf} in the heatwave treatment (Figure 5b) but failed to predict the maintenance of relatively high E_{canopy} at T_{leaf} values exceeding 40°C (Figure 5d). We also compared the

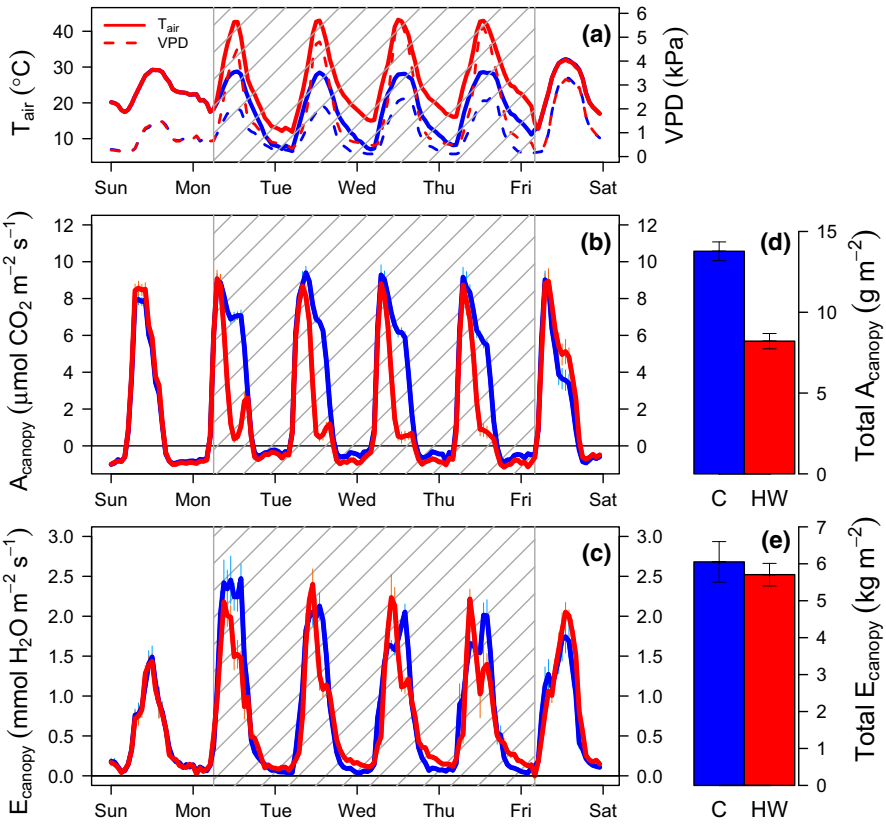

FIGURE 2 Time course of canopy CO_2 uptake and water loss in response to an experimental 4-day heatwave. Air temperature and vapor pressure deficit (VPD; a) canopy-scale measurements of CO_2 uptake (A_{canopy}; b) and H_2O loss (E_{canopy}; c) during an extreme heatwave treatment. The shaded area denotes when six heatwave trees were exposed to 4 days with a maximum air temperature of 43–44°C, while the six control trees experienced a maximum air temperature of 28–29°C. A_{canopy} and E_{canopy} fluxes are expressed per unit leaf area. Thick solid lines reflect the mean and thin vertical lines reflect the standard error (n = 6). Fluxes were summed over the 4-day heatwave for A_{canopy} (d) and E_{canopy} (e); error bars reflect the standard error (n = 6)

predictions of two widely used stomatal models (Ball et al., 1987; Leuning, 1995), which yielded nearly identical results (Figures S10–S11). These models, consistent with photosynthetic schemes used in global land models, assume a positive functional link between photosynthesis and g_s such that predicted E_{canopy} declines toward zero as photosynthesis declines to zero. By contrast, our observations suggest that this link between photosynthesis and g_s was decoupled under the extreme heatwave conditions. Under heatwave conditions, observed T_{leaf} was up to 7.5°C cooler than predicted by the model (mean of 2.8°C, range of 0.1–7.5°C cooler; Figure 3b). Thus, continued latent cooling during the extreme heatwave moderated T_{leaf} and enabled the maintenance of T_{leaf} below T_{50} (Figure 4).

The heatwave treatment did not negatively affect the hydraulic system of these trees. Predawn and midday leaf water potentials were maintained at moderate values that were less negative than the TLP in all treatments (Figure S6). The most extreme observed leaf water potential values were approximately −2.0 MPa, which is less negative than the water potential at which similar *Eucalyptus* species begin to lose hydraulic conductivity (approximately −3.5 MPa; Bourne, Creek, Peters, Ellsworth, & Choat, 2017). Branch hydraulic conductivity was not strongly impaired by emboli before or after the heatwave (Figure S7a). Furthermore, leaf hydraulic conductance on the fourth day of the heatwave was equivalently high across all treatments (Figure S7b). This occurred even with low soil water content (Figure S1); trees acquired water from across the soil profile during the heatwave and particularly from 30 to 150 cm depth (Figures S1–S2).

The heatwave did not cause widespread canopy damage or growth reductions. We observed some leaf browning, potentially indicative of acute thermal damage, but these symptoms were rare and affected just 1.1% of the leaf area of heatwave trees compared with 0.3% for control trees (Figure S8). We observed no tree mortality, and trajectories of diameter and height growth were not affected by the heatwave (Figure S9).

4 | DISCUSSION

These trees successfully coped with an extreme heatwave despite dry surface soils and exceptionally hot and dry atmospheric conditions. We documented an integrative physiological response to the

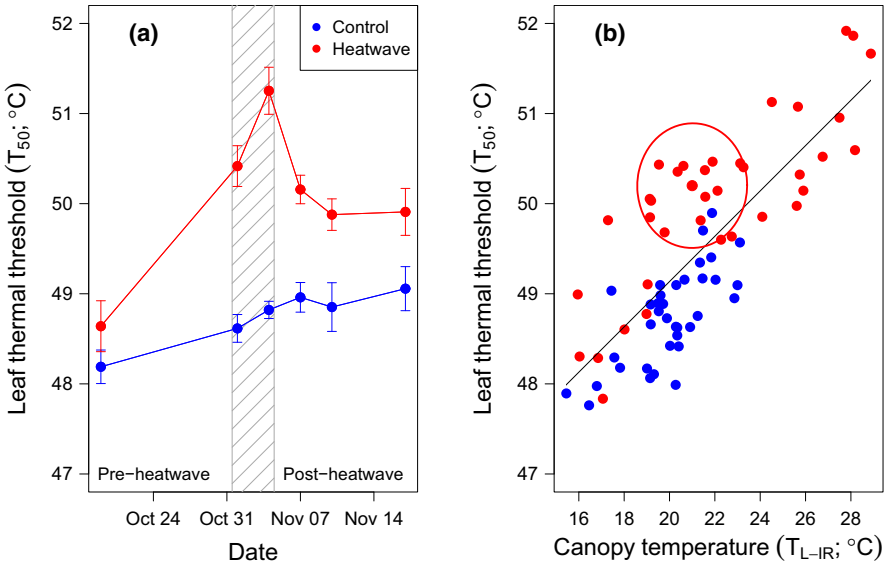

FIGURE 3 Thermal tolerance and temperature of leaves during an extreme experimental heatwave in the Austral Spring–Summer. The leaf high-temperature thermal threshold (T_{50}) strongly increased in response to the heatwave treatment (a); symbols reflect the mean and error bars reflect 1SE ($n = 6$). The shaded area denotes an extreme 4-day heatwave treatment. The change in T_{50} over time was correlated with the average measured canopy temperature of the preceding 24 hr (b). The solid line was fit to all of the data ($y = 44.1 + 0.25x$, $r^2 = .61$, $p < .001$). This relationship had a counterclockwise hysteresis, as the heatwave trees maintained higher T_{50} than expected on the postheatwave days (red circle)

heatwave that included substantial latent cooling of leaves despite net photosynthetic rates of approximately zero, the maintenance of a healthy and functional hydraulic system, and increased leaf thermal tolerance such that leaf temperatures did not exceed the upper thermal limit (T_{50}). These mechanisms are relevant to our understanding of tree tolerance to extreme heat waves and to model predictions of future heatwave intensity at landscape and global scales.

4.1 | Photosynthetic decoupling

There is abundant evidence that photosynthesis and stomatal conductance are strongly coupled under most environmental conditions (Farquhar & Sharkey, 1982; Lin et al., 2015; Wong, Cowan, & Farquhar, 1979), and that mathematical models based on this coupling more accurately describe observed data (De Kauwe et al., 2013; Duursma et al., 2014; Rogers et al., 2017). Given this evidence, nearly all mathematical models of C cycling implement a positive functional link between stomatal conductance and photosynthetic rates (Ball et al., 1987; Leuning, 1995; Medlyn et al., 2011). Our observations suggest that this link between photosynthesis and g_s was decoupled under the extreme heatwave conditions. We emphasize, however, that g_s must have declined with increasing temperature during the experimental heatwave, or canopy transpiration would have increased strongly in response to rising VPD. However, g_s did not decline as strongly as predicted by the photosynthetic models.

Photosynthetic decoupling is consistent with some recent studies with potted plants in controlled conditions (Ameye et al., 2012; von Caemmerer & Evans, 2015; Slot, Garcia, & Winter, 2016; Urban et al., 2017). For example, Urban et al. (2017) found that increasing temperature was associated with increased g_s for potted trees exposed to low VPD and high soil moisture, despite zero or negative rates of photosynthesis. Slot et al. (2016) found that g_s declined with temperature up to ~42°C, but that g_s subsequently increased at higher temperatures, despite zero or negative photosynthetic rates. Given the evidence presented here and in these recent reports, we suggest that latent cooling of leaves by transpiration is an important component to plant response to extreme temperatures that is not incorporated into our current models of photosynthesis (Rogers et al., 2017). We acknowledge that alternative photosynthetic model formulations exist that specifically incorporate plant hydraulics to simulate stomatal closure to maintain moderate leaf water potentials (Bonan, Williams, Fisher, & Oleson, 2014; Tuzet, Perrier, & Leuning, 2003). Such formulations may be able to be modified to allow for photosynthetic uncoupling similar to that observed here, with additional constraints imposed by the water potential gradient from the soil to the atmosphere.

4.2 | Thermal tolerance

O'Sullivan et al. (2017) recently published a global synthesis of leaf thermal tolerance for 218 species, noting that most plants have a large safety margin between maximum environmental temperatures and the leaf upper thermal limit. They also demonstrated acclimation in leaf thermal tolerance of ~0.3°C per 1.0°C increase in growth temperature using repeated measurements of six species in contrasting warm and cool seasons. This observation has been subsequently confirmed for 62 species across Australia (Zhu et al., 2018). O'Sullivan et al. (2017) argue, however, that

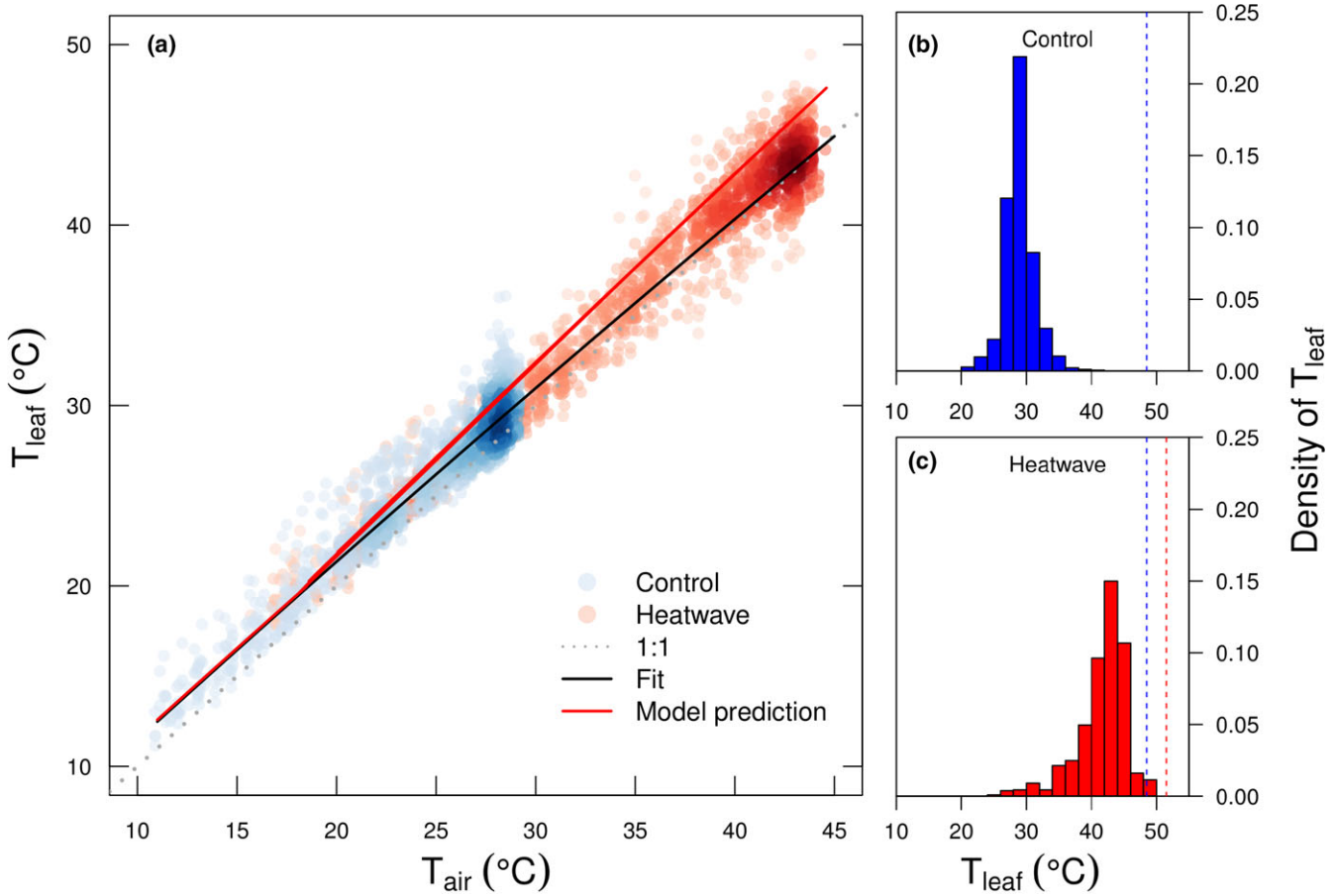

FIGURE 4 The temperature of leaves during an extreme experimental heatwave in the Austral Spring–Summer. Leaf temperature (T_{leaf}) measured in the upper canopy of each tree was strongly correlated with air temperature (T_{air}; a). Points reflect 15 min averages of data collected during high light conditions (PPFD > 500 μmol m^{-2} s^{-1}) from October 31, 2016 to November 3, 2016. The dashed line shows 1:1, the solid black line was fit to the data: (T_{leaf} = 1.38 + 1.02 * T_{air} − 0.0012 * T_{air}^2, $p < .001$, $r^2 = .8$), and the solid red line shows the predicted leaf temperatures by the photosynthetic model. Histograms of T_{leaf} in high light conditions (PPFD > 500 μmol m^{-2} s^{-1}, 12–16 hr) in control and heatwave treatments (b–c) were constrained to values below T_{50}. The T_{50} values are shown as the vertical dashed lines (b–c; blue = control or before heatwave T_{50}, red = peak heatwave T_{50}). Note that some leaves in the heatwave treatment exceeded the T_{50} value observed preheatwave (dashed blue line) but did not exceed the T_{50} value observed during the heatwave (dashed red line; c)

increasing heatwave intensity will likely shrink this thermal safety margin and put some species at risk of thermal damage in the future, particularly in midlatitude regions where heatwave intensities are highest. This was true even when accounting for acclimation in thermal tolerance, as the predicted increases in heatwave temperatures exceeded the predicted increase in thermal tolerance. Our study confirms that the upper thermal limit of leaf function is not a fixed trait, and that at least some plants are capable of large and rapid adjustments in this upper thermal limit that likely contributes to heatwave tolerance. The increase in thermal tolerance reported here (~0.25°C per 1.0°C change in average leaf temperature; Figure 3b) is broadly consistent with the seasonal change reported by O'Sullivan et al. (2017) and Zhu et al. (2018), confirming that acclimation of leaf thermal tolerance mitigates some of the risk associated with future heatwaves. Possible limits to the adjustment of leaf thermal tolerance remain a key unknown for future research.

4.3 | Interactions with water availability

These trees continued substantial latent cooling via transpiration during this heatwave (average cooling of 2.8°C). We note, however, that this latent cooling is contingent on soil water availability (van Gorsel et al., 2016; Urban et al., 2017). These *Eucalyptus* trees continued to access soil water without loss of hydraulic function despite low surface soil moisture and a lack of recent precipitation, but shallow or very dry soils may preclude this response in some systems (van Gorsel et al., 2016; Teskey et al., 2015). *Eucalyptus* trees are known to be facultative users of deep soil water and groundwater (Eamus, Zolfaghar, Villalobos-Vega, Cleverly, & Huete, 2015; O'Grady, Eamus, & Hutley, 1999). Shallow-rooting species without access to groundwater may not be capable of continued latent cooling during a heatwave that follows a month without precipitation. We speculate that trees without groundwater access rely primarily on physical adaptations such as reflective leaves (Curtis, Leigh, &

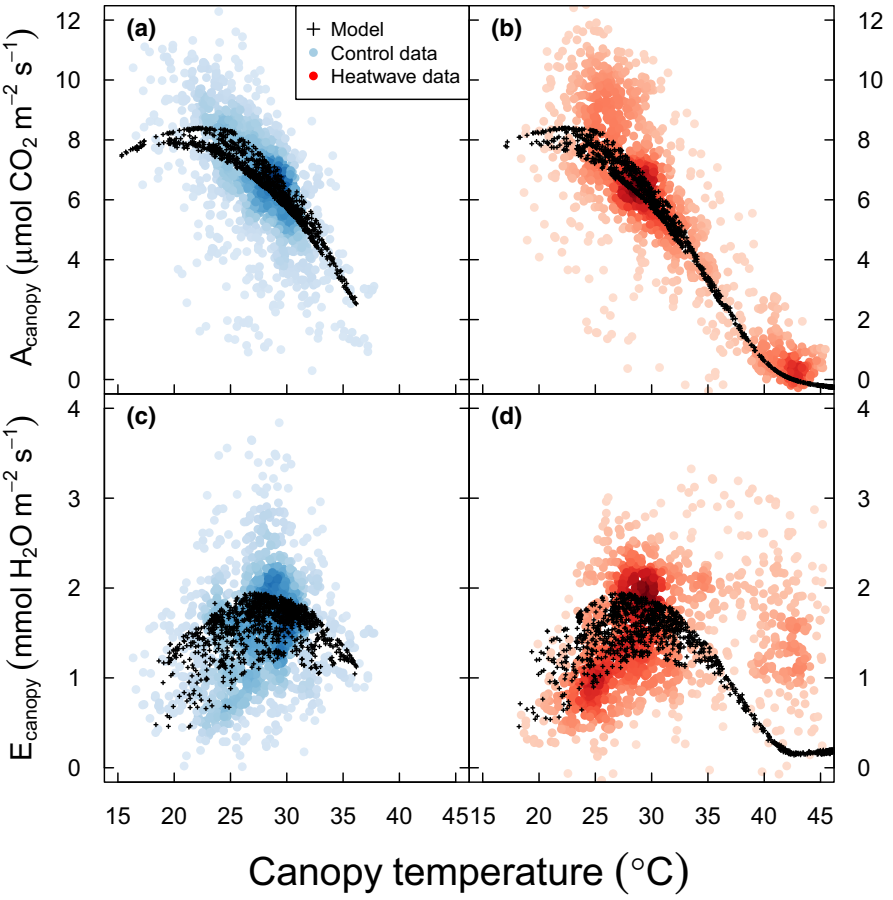

FIGURE 5 Canopy-scale measurements of leaf photosynthesis (A_{canopy}) and transpiration (E_{canopy}) compared with the predictions of a photosynthetic model. Observed data are shown as density plots, with darker colors for areas of more frequent observations. The model was fit to the A_{canopy} and E_{canopy} data in the control treatment (a, c). This model suitably predicted the observed decline in A_{canopy} in the heatwave treatment (b). However, the model predicts strong stomatal closure and reduction in E_{canopy} toward zero above 40°C in the heatwave treatment, while observed E_{canopy} fluxes remained moderately high (d)

Rayburg, 2012; Ehleringer & Mooney, 1978) or biochemical adaptations such as heat-shock proteins (Feder & Hofmann, 1999) to cope with extreme heatwaves. The interplay between these adaptations and latent cooling may be an interesting area of further study (e.g., Lin, Chen, Zhang, Fu, & Fan, 2017).

4.4 | Implications for modeling

The latent cooling of transpiration was substantial during this heatwave, with an average cooling of 2.8°C up to an extreme of 7.5°C, and T_{leaf} was maintained at moderate values below the upper thermal limit for leaf function. The earth system models used to predict the incidence and biological impact of future heatwaves do not currently incorporate this mechanism, although recent work would suggest that such latent cooling could impact heatwave intensity in terms of land surface air temperatures at large spatial scales. For example, Kala et al. (2016) implemented an alternative stomatal conductance scheme (Lin et al., 2015; Medlyn et al., 2011) into an earth system model, leading to large increases (4–5°C) in the predicted values of maximum air temperature in Western Europe and Asia. However, high latent cooling of a forested landscape has the potential to moderate heatwave intensity, suggesting that this mechanism should be explored in model projections of land surface temperatures in future heatwaves (Cowan et al., 2014; Kala et al., 2016; Li & Bou-Zeid, 2013; Sillmann et al., 2013).

Latent cooling during heatwave events is also relevant to urban forestry and the design of green cities. A recent model analysis suggested that urban trees in 10 megacities provided valuable human benefits, including mitigation of the urban heat island effect and reduced cooling expenses for buildings (Endreny et al., 2017). Designing cities to incorporate tree cover may ameliorate heatwave intensity and contribute positively to human health outcomes (Li & Bou-Zeid, 2013).

5 | CONCLUSION

We performed an extreme heatwave experiment with field grown and relatively large *Eucalypts parramattensis* trees. The trees exhibited a coordinated physiological response utilizing latent cooling and

a rapid increase in leaf thermal thresholds, such that the trees experienced little thermal damage and no observable decline in growth. We conclude that this tree species was remarkably capable of tolerating an extreme heatwave via mechanisms that have implications for future heatwave intensity and forest resilience in a warmer world.

ACKNOWLEDGEMENTS

We thank Burhan Amiji (Western Sydney University) for maintaining the site and for his excellent research support. We thank Alicia Cook (University of Technology Sydney) for her guidance on the T_{50} measurements. This experiment was made possible through a collaboration with Sune Linder and the Swedish University of Agricultural Sciences, who designed, built, and generously provided the whole tree chambers. We also gratefully acknowledge Renee Smith, Carrie Drake (Western Sydney University), and Richard Harwood (Sydney University) for their help with the whole-tree harvests. We thank Marlies Kovenock (University of Washington) and three anonymous reviewers for useful suggestions on a previous version of this manuscript. This research was supported by the Australian Research Council (Discovery, DP140103415), a New South Wales government Climate Action Grant (NSW T07/CAG/016), the Hawkesbury Institute for the Environment, and Western Sydney University.

AUTHOR CONTRIBUTION

JED co-led the experimental design, contributed to data collection for the chamber flux, T_{50}, and T_{leaf} datasets, coordinated the experimental implementation, and led the data analysis, modeling, and writing. MGT was the senior scientific lead; he co-led the experimental design and made large contributions to analysis, interpretation, and writing. AV led the T_{50} and T_{leaf} data collection and contributed to the experimental design, data analysis, and writing. BEM made a large contribution to the modeling component and contributed to the experimental design, interpretation, and writing. PBR contributed to the experimental design, interpretation, and writing. AL contributed to the experimental design, T_{50} measurements, interpretation, and writing. SP co-led the hydraulic measurements and contributed to experimental design, data analysis, interpretation, and writing. CJB co-led the hydraulic measurements and contributed to data analysis, interpretation, and writing. RL co-led the hydraulic measurements and contributed to data analysis, interpretation, and writing. MJA contributed to the experimental design, interpretation, and writing. KYC contributed to the T_{50} and T_{leaf} measurements, experimental design, and writing. RAD contributed to the modeling component, experimental design, interpretation, and writing. DK contributed to the modeling component, interpretation, and writing. MGD contributed to the modeling component, interpretation, and writing. MJ contributed to the modeling component, interpretation, and writing. ABN contributed to the T_{50} measurements and contributed to interpretation and writing. DTT contributed to the hydraulics measurements, experimental design, and writing. BC contributed to the hydraulics measurements and writing. OKA contributed to interpretation and writing. CVMB contributed to the measurements of chamber flux and leaf temperature and contributed to experimental design, data analysis, and writing.

ORCID

John E. Drake http://orcid.org/0000-0003-1758-2169
Mark G. Tjoelker http://orcid.org/0000-0003-4607-5238
Belinda E. Medlyn http://orcid.org/0000-0001-5728-9827
Andrea Leigh http://orcid.org/0000-0003-3568-2606
Sebastian Pfautsch http://orcid.org/0000-0002-4390-4195
Michael J. Aspinwall http://orcid.org/0000-0003-0199-2972
Kristine Y. Crous http://orcid.org/0000-0001-9478-7593
Remko A. Duursma http://orcid.org/0000-0002-8499-5580
Martin G. De Kauwe http://orcid.org/0000-0002-3399-9098
Mingkai Jiang http://orcid.org/0000-0002-9982-9518
Adrienne B. Nicotra http://orcid.org/0000-0001-6578-369X
David T. Tissue http://orcid.org/0000-0002-8497-2047
Brendan Choat http://orcid.org/0000-0002-9105-640X
Owen K. Atkin http://orcid.org/0000-0003-1041-5202

REFERENCES

Allen, C. D., Breshears, D. D., & McDowell, N. G. (2015). On underestimation of global vulnerability to tree mortality and forest die-off from hotter drought in the Anthropocene. *Ecosphere*, *6*, 129. https://doi.org/10.1890/ES15-00203.1

Allen, C. D., Macalady, A. K., Chenchouni, H., Bachelet, D., McDowell, N., Vennetier, M., … Gonzalez, P. (2010). A global overview of drought and heat-induced tree mortality reveals emerging climate change risks for forests. *Forest Ecology and Management*, *259*, 660–684. https://doi.org/10.1016/j.foreco.2009.09.001

Ameye, M., Wertin, T. M., Bauweraerts, I., McGuire, M. A., Teskey, R. O., & Steppe, K. (2012). The effect of induced heat waves on *Pinus taeda* and *Quercus rubra* seedlings in ambient and elevated CO_2 atmospheres. *New Phytologist*, *196*, 448–461. https://doi.org/10.1111/j.1469-8137.2012.04267.x

Aspinwall, M. J., Drake, J. E., Campany, C., Vårhammar, A., Ghannoum, O., Tissue, D. T., … Tjoelker, M. G. (2016). Convergent acclimation of leaf photosynthesis and respiration to prevailing ambient temperatures under current and warmer climates in *Eucalyptus tereticornis*. *New Phytologist*, *212*, 354–367. https://doi.org/10.1111/nph.14035

Australian Bureau of Meteorology State of the Climate Report. (2016).

Ball, J., Woodrow, I., & Berry, J. A. (1987). A model predicting stomatal conductance and its contribution to the control of photosynthesis under different environmental conditions. In *Progress in Photosynthesis Research*, Vol. *IV* (pp. 221–224). Dordrecht, The Netherlands: Martinus-Nijhoff Publishers. https://doi.org/10.1007/978-94-017-0519-6

Barton, C. V. M., Ellsworth, D. S., Medlyn, B. E., Duursma, R. A., Tissue, D. T., Adams, M. A., … Linder, S. (2010). Whole-tree chambers for elevated atmospheric CO_2 experimentation and tree scale flux measurements in south-eastern Australia: The Hawkesbury Forest Experiment. *Agricultural and Forest Meteorology*, *150*, 941–951. https://doi.org/10.1016/j.agrformet.2010.03.001

Bonan, G. B., Williams, M., Fisher, R. A., & Oleson, K. W. (2014). Modeling stomatal conductance in the earth system: Linking leaf water-use

efficiency and water transport along the soil–plant–atmosphere continuum. *Geoscientific Model Development*, *7*, 2193–2222. https://doi.org/10.5194/gmd-7-2193-2014

Bourne, A. E., Creek, D., Peters, J. M. R., Ellsworth, D. S., & Choat, B. (2017). Species climate range influences hydraulic and stomatal traits in Eucalyptus species. *Annals of Botany*, *120*, 123–133. https://doi.org/10.1093/aob/mcx020

Brodribb, T. J., & Holbrook, N. M. (2003). Stomatal closure during leaf dehydration, correlation with other leaf physiological traits. *Plant Physiology*, *132*, 2166–2173. https://doi.org/10.1104/pp.103.023879

von Caemmerer, S., & Evans, J. R. (2015). Temperature responses of mesophyll conductance differ greatly between species. *Plant, Cell & Environment*, *38*, 629–637. https://doi.org/10.1111/pce.12449

Ciais, P., Reichstein, M., Viovy, N., Granier, A., Ogée, J., Allard, V., … Chevallier, F. (2005). Europe-wide reduction in primary productivity caused by the heat and drought in 2003. *Nature*, *437*, 529–533. https://doi.org/10.1038/nature03972

Colombo, S. J., & Timmer, V. R. (1992). Limits of tolerance to high temperatures causing direct and indirect damage to black spruce. *Tree Physiology*, *11*, 95–104. https://doi.org/10.1093/treephys/11.1.95

Cowan, T., Purich, A., Perkins, S., Pezza, A., Boschat, G., & Sadler, K. (2014). More frequent, longer, and hotter heat waves for Australia in the Twenty-First Century. *Journal of Climate*, *27*, 5851–5871. https://doi.org/10.1175/JCLI-D-14-00092.1

Curtis, E. M., Knight, C. A., Petrou, K., & Leigh, A. (2014). A comparative analysis of photosynthetic recovery from thermal stress: A desert plant case study. *Oecologia*, *175*, 1051–1061. https://doi.org/10.1007/s00442-014-2988-5

Curtis, E. M., Leigh, A., & Rayburg, S. (2012). Relationships among leaf traits of Australian arid zone plants: Alternative modes of thermal protection. *Australian Journal of Botany*, *60*, 471–483. https://doi.org/10.1071/BT11284

De Kauwe, M. G., Medlyn, B. E., Zaehle, S., Walker, A. P., Dietze, M. C., Hickler, T., … Smith, B. (2013). Forest water use and water use efficiency at elevated CO_2: A model-data intercomparison at two contrasting temperate forest FACE sites. *Global Change Biology*, *19*, 1759–1779. https://doi.org/10.1111/gcb.12164

Drake, J. E., Tjoelker, M. G., Aspinwall, M. J., Reich, P. B., Barton, C. V. M., Medlyn, B. E., & Duursma, R. A. (2016). Does physiological acclimation to climate warming stabilize the ratio of canopy respiration to photosynthesis? *New Phytologist*, *211*, 850–863. https://doi.org/10.1111/nph.13978

Duursma, R. A. (2015). Plantecophys—an r package for analysing and modelling leaf gas exchange data. *PLoS ONE*, *10*, e0143346. https://doi.org/10.1371/journal.pone.0143346

Duursma, R. A., Barton, C. V. M., Eamus, D., Medlyn, B. E., Ellsworth, D. S., Forster, M. A., … McMurtrie, R. E. (2011). Rooting depth explains $[CO_2]$ × drought interaction in Eucalyptus saligna. *Tree Physiology*, *31*, 922–931. https://doi.org/10.1093/treephys/tpr030

Duursma, R. A., Barton, C. V. M., Lin, Y.-S., Medlyn, B. E., Eamus, D., Tissue, D. T., … McMurtrie, R. E. (2014). The peaked response of transpiration rate to vapour pressure deficit in field conditions can be explained by the temperature optimum of photosynthesis. *Agricultural and Forest Meteorology*, *189*, 2–10. https://doi.org/10.1016/j.agrformet.2013.12.007

Eamus, D., Zolfaghar, S., Villalobos-Vega, R., Cleverly, J., & Huete, A. (2015). Groundwater-dependent ecosystems: Recent insights from satellite and field-based studies. *Hydrology and Earth System Sciences*, *19*, 4229–4256. https://doi.org/10.5194/hess-19-4229-2015

Ehleringer, J. R., & Mooney, H. A. (1978). Leaf hairs: Effects on physiological activity and adaptive value to a desert shrub. *Oecologia*, *37*, 183–200. https://doi.org/10.1007/BF00344990

Endreny, T., Santagata, R., Perna, A., Stefano, C. D., Rallo, R. F., & Ulgiati, S. (2017). Implementing and managing urban forests: A much needed conservation strategy to increase ecosystem services and urban wellbeing. *Ecological Modelling*, *360*, 328–335. https://doi.org/10.1016/j.ecolmodel.2017.07.016

Farquhar, G. D., Caemmerer, S. V., & Berry, J. A. (1980). A biochemical model of photosynthetic CO_2 assimilation in leaves of C3 species. *Planta*, *149*, 78–90. https://doi.org/10.1007/BF00386231

Farquhar, G., & Sharkey, T. (1982). Stomatal conductance and photosynthesis. *Annual Review of Plant Physiology and Plant Molecular Biology*, *33*, 317–345. https://doi.org/10.1146/annurev.pp.33.060182.001533

Feder, M. E., & Hofmann, G. E. (1999). Heat-shock proteins, molecular chaperones, and the stress response: Evolutionary and ecological physiology. *Annual Review of Physiology*, *61*, 243–282. https://doi.org/10.1146/annurev.physiol.61.1.243

Frank, D., Reichstein, M., Bahn, M., Thonicke, K., Frank, D., Mahecha, M. D., … Beer, C. (2015). Effects of climate extremes on the terrestrial carbon cycle: Concepts, processes and potential future impacts. *Global Change Biology*, *21*, 2861–2880. https://doi.org/10.1111/gcb.12916

Gifford, D. J., & Taleisnik, E. (1994). Heat-shock response of Pinus and Picea seedlings. *Tree Physiology*, *14*, 103–110. https://doi.org/10.1093/treephys/14.1.103

van Gorsel, E., Wolf, S., Cleverly, J., Isaac, P., Haverd, V., Ewenz, C. M., … Griebel, A. (2016). Carbon uptake and water use in woodlands and forests in southern Australia during an extreme heat wave event in the "Angry Summer" of 2012/2013. *Biogeosciences*, *13*, 5947–5964. https://doi.org/10.5194/bg-13-5947-2016

Hansen, J., Sato, M., & Ruedy, R. (2012). Perception of climate change. *Proceedings of the National Academy of Sciences of the United States of America*, *109*, E2415–E2423. https://doi.org/10.1073/pnas.1205276109

IPCC (2014). *Climate Change 2014: Synthesis Report*. Geneva, Switzerland: IPCC.

Kala, J., De Kauwe, M. G., Pitman, A. J., Medlyn, B. E., Wang, Y.-P., Lorenz, R., & Perkins-Kirkpatrick, S. E. (2016). Impact of the representation of stomatal conductance on model projections of heatwave intensity. *Scientific Reports*, *6*, 23418. https://doi.org/10.1038/srep23418

Leuning, R. (1995). A critical-appraisal of a combined stomatal-photosynthesis model for C-3 plants. *Plant Cell and Environment*, *18*, 339–355. https://doi.org/10.1111/j.1365-3040.1995.tb00370.x

Li, D., & Bou-Zeid, E. (2013). Synergistic interactions between urban heat islands and heat waves: The impact in cities is larger than the sum of its parts*. *Journal of Applied Meteorology and Climatology*, *52*, 2051–2064. https://doi.org/10.1175/JAMC-D-13-02.1

Lin, H., Chen, Y., Zhang, H., Fu, P., & Fan, Z. (2017). Stronger cooling effects of transpiration and leaf physical traits of plants from a hot dry habitat than from a hot wet habitat. *Functional Ecology*, *31*, 2202–2211.

Lin, Y.-S., Medlyn, B. E., Duursma, R. A., Prentice, I. C., Wang, H., Baig, S., … De Beeck, M. O. (2015). Optimal stomatal behaviour around the world. *Nature Climate Change*, *5*, 459–464. https://doi.org/10.1038/nclimate2550

Lin, Y.-S., Medlyn, B. E., & Ellsworth, D. S. (2012). Temperature responses of leaf net photosynthesis: The role of component processes. *Tree Physiology*, *32*, 219–231. https://doi.org/10.1093/treephys/tpr141

Medlyn, B. E., Duursma, R. A., Eamus, D., Ellsworth, D. S., Prentice, I. C., Barton, C. V., … Wingate, L. (2011). Reconciling the optimal and empirical approaches to modelling stomatal conductance. *Global Change Biology*, *17*, 2134–2144. https://doi.org/10.1111/j.1365-2486.2010.02375.x

Mitchell, P. J., O'Grady, A. P., Hayes, K. R., & Pinkard, E. A. (2014). Exposure of trees to drought-induced die-off is defined by a common climatic threshold across different vegetation types. *Ecology and Evolution*, *4*, 1088–1101. https://doi.org/10.1002/ece3.1008

O'Grady, A. P., Eamus, D., & Hutley, L. B. (1999). Transpiration increases during the dry season: Patterns of tree water use in eucalypt open-forests of northern Australia. *Tree Physiology*, *19*, 591–597. https://doi.org/10.1093/treephys/19.9.591

O'Sullivan, O. S., Heskel, M. A., Reich, P. B., Tjoelker, M. G., Weerasinghe, L. K., Penillard, A., ... Bahar, N. H. (2017). Thermal limits of leaf metabolism across biomes. *Global Change Biology*, *23*, 209–223. https://doi.org/10.1111/gcb.13477

Phillips, S., Callaghan, J., & Thompson, V. (2000). The tree species preferences of koalas (*Phascolarctos cinereus*) inhabiting forest and woodland communities on Quaternary deposits in the Port Stephens area, New South Wales. *Wildlife Research*, *27*, 1–10. https://doi.org/10.1071/WR98054

Reich, P. B., Sendall, K. M., Stefanski, A., Wei, X., Rich, R. L., & Montgomery, R. A. (2016). Boreal and temperate trees show strong acclimation of respiration to warming. *Nature*, *531*, 633–+. https://doi.org/10.1038/nature17142

Reichstein, M., Bahn, M., Ciais, P., Frank, D., Mahecha, M. D., Seneviratne, S. I., ... Papale, D. (2013). Climate extremes and the carbon cycle. *Nature*, *500*, 287–295. https://doi.org/10.1038/nature12350

Rogers, A., Medlyn, B. E., Dukes, J. S., Bonan, G., Caemmerer, S., Dietze, M. C., ... Prentice, I. C. (2017). A roadmap for improving the representation of photosynthesis in Earth system models. *New Phytologist*, *213*, 22–42. https://doi.org/10.1111/nph.14283

Sillmann, J., Kharin, V. V., Zwiers, F. W., Zhang, X., & Bronaugh, D. (2013). Climate extremes indices in the CMIP5 multimodel ensemble: Part 2. Future climate projections. *Journal of Geophysical Research-Atmospheres*, *118*, 2473–2493. https://doi.org/10.1002/jgrd.50188

Slot, M., Garcia, M. N., & Winter, K. (2016). Temperature response of CO_2 exchange in three tropical tree species. *Functional Plant Biology*, *43*, 468–478.

Smith, N. G., & Dukes, J. S. (2013). Plant respiration and photosynthesis in global-scale models: Incorporating acclimation to temperature and CO_2. *Global Change Biology*, *19*, 45–63. https://doi.org/10.1111/j.1365-2486.2012.02797.x

Teskey, R., Wertin, T., Bauweraerts, I., Ameye, M., McGuire, M. A., & Steppe, K. (2015). Responses of tree species to heat waves and extreme heat events. *Plant Cell and Environment*, *38*, 1699–1712. https://doi.org/10.1111/pce.12417

Tuzet, A., Perrier, A., & Leuning, R. (2003). A coupled model of stomatal conductance, photosynthesis and transpiration. *Plant, Cell & Environment*, *26*, 1097–1116. https://doi.org/10.1046/j.1365-3040.2003.01035.x

Tyree, M. T., & Hammel, H. T. (1972). The measurement of the turgor pressure and the water relations of plants by the pressure-bomb technique. *Journal of Experimental Botany*, *23*, 267–282. https://doi.org/10.1093/jxb/23.1.267

Urban, J., Ingwers, M. W., McGuire, M. A., & Teskey, R. O. (2017). Increase in leaf temperature opens stomata and decouples net photosynthesis from stomatal conductance in Pinus taeda and *Populus deltoides* × nigra. *Journal of Experimental Botany*, *68*, 1757–1767. https://doi.org/10.1093/jxb/erx052

Wang, Y. P., & Leuning, R. (1998). A two-leaf model for canopy conductance, photosynthesis and partitioning of available energy I: Model description and comparison with a multi-layered model. *Agricultural and Forest Meteorology*, *91*, 89–111. https://doi.org/10.1016/S0168-1923(98)00061-6

Wong, S. C., Cowan, I. R., & Farquhar, G. D. (1979). Stomatal conductance correlates with photosynthetic capacity. *Nature*, *282*, 424–426. https://doi.org/10.1038/282424a0

Yamori, W., Hikosaka, K., & Way, D. A. (2014). Temperature response of photosynthesis in C-3, C-4, and CAM plants: Temperature acclimation and temperature adaptation. *Photosynthesis Research*, *119*, 101–117. https://doi.org/10.1007/s11120-013-9874-6

Yuan, W., Cai, W., Chen, Y., Liu, S., Dong, W., Zhang, H., ... Liu, D. (2016). Severe summer heatwave and drought strongly reduced carbon uptake in Southern China. *Scientific Reports*, *6*, srep18813. https://doi.org/10.1038/srep18813

Zhu, L., Bloomfield, K. J., Hocart, C. H., Egerton, J. J. G., O'Sullivan, O. S., Penillard, A., ... Atkin, O. K. (2018). Plasticity of photosynthetic heat tolerance in plants adapted to thermally contrasting biomes. *Plant Cell & Environment*. https://doi.org/10.1111/pce.13133. [Epub ahead of print]

SUPPORTING INFORMATION

Additional Supporting Information may be found online in the supporting information tab for this article.

How to cite this article: Drake JE, Tjoelker MG, Vårhammar A, et al. Trees tolerate an extreme heatwave via sustained transpirational cooling and increased leaf thermal tolerance. *Glob Change Biol*. 2018;00:1–13. https://doi.org/10.1111/gcb.14037

Graphical Abstract

The contents of this page will be used as part of the graphical abstract of html only.
It will not be published as part of main article.

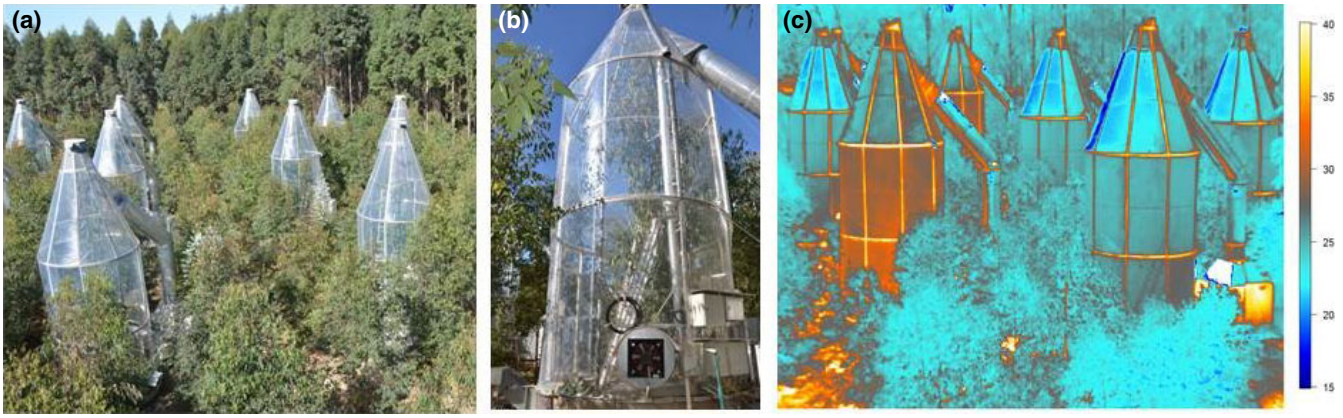

Heatwaves are likely to increase in frequency and intensity, but we know relatively little about how trees will respond. Here, we documented that large trees growing in the field responded to an extreme heatwave with a coordinated physiological response involving continued leaf cooling from transpiration and a rapid increase in leaf thermal tolerance. The Eucalyptus trees that we studied were remarkably capable of tolerating an extreme heatwave via mechanisms that have implications for future heatwave intensity and forest resilience in a warmer world.